Challenge Journal of Structural Mechanics

Research Article

The mechanical properties of cement mortar reinforced with silica fume subjected to sulfate and chloride environment

Sulaiman Al-Safi [a], Abdulghani Altharehi [a,*], Ibrahim A. Alameri [a], Abdulmalek Al-Jolahy [a]

[a] *Department of Civil Engineering, Sana'a University, 13341 Sana'a, Yemen*

ABSTRACT

This study investigates the effect of incorporating micro-sized silica fume on the mechanical properties and durability of cement mortar when exposed to sulfate and chloride environments. Mortar samples were prepared by replacing cement with micro-sized silica fume in varying proportions of 5%, 10%, 15%, 20%, 25%, 30%, and 35% by weight. The specimens were cured in water and chemically aggressive conditions, including 5% and 10% sodium sulfate solutions, as well as mixtures of 5% and 10% sodium chloride solutions, to simulate real-world exposure to such environments. Experimental results revealed that the addition of silica fume significantly enhanced the mortar's resistance to chemical deterioration caused by sulfates and chlorides. This improvement is attributed to the pozzolanic reaction of silica fume, which contributed to denser microstructures, reduced porosity, and a stronger bond within the matrix. Among the tested proportions, the optimal replacement ratios for achieving the best balance between mechanical strength and durability were identified up to 20%. These findings highlight the efficiency of silica fume as a supplementary cementitious material in mitigating the adverse effects of aggressive chemical agents. Such modifications can be particularly valuable in improving the service life of concrete structures exposed to harsh environmental conditions, enhancing sustainability and cost-effectiveness in construction practices.

ARTICLE INFO

Article history:
Received – November 5, 2024
Revision requested – December 23, 2024
Revision received – January 13, 2025
Accepted – January 21, 2025

Keywords:
Cement mortar
Silica fume
Sulfate attack
Chloride attack
Reactivity

Citation: Al-Safi S, Altharehi A, Alameri IA, Al-Jolahy A (2025). The mechanical properties of cement mortar reinforced with silica fume subjected to sulfate and chloride environment. *Challenge Journal of Structural Mechanics*, 11(1), 55–69.

1. Introduction

Although concrete is widely recognized for its strength and durability, it is susceptible to environmental factors that can degrade its integrity over time (Alameri et al. 2020). Among these, sulphate and chloride attacks are particularly insidious. Sulfate ions, common in some soils and groundwater, initiate expansive chemical reactions within the concrete matrix, leading to cracking and deterioration. Chloride ions, on the other hand, often originating from de-icing salts or marine environments, penetrate the concrete to corrode its steel reinforcement and weaken micro-structural stability. Acid attacks typically result from various industrial processes and related applications (Atabey et al. 2023).

Pozzolans have long been recognized as vital supplementary materials in enhancing the performance and durability of concrete (Saif Allah et al. 2024). These materials, including natural pozzolans such as fly ash (Harirchian 2024), silica fume (Güney and Yıldızel 2024), and volcanic ash (Atasever and Tokyay 2024), are widely utilized to improve the longevity of concrete structures (McCarthy and Dyer 2019). By refining the microstructure and reducing permeability, pozzolans effectively limit the ingress of aggressive sulfate and chloride ion (Anwar 2005). This significantly reduces the risk of chloride-induced corrosion in steel reinforcement. Additionally, certain pozzolans, such as silica fume, possess unique properties that further enhance the overall performance of concrete. (Feng et al. 2018).

* *Corresponding author*. E-mail address: a.altharhi@su.edu.ye (A. Altharehi)
ISSN: 2149-8024 / DOI: https://doi.org/10.20528/cjsmec.2025.01.005

Silica fume, which is rich in silicon dioxide, enhances the durability of concrete by improving its resistance to sulfate and chloride attacks (Şimşek et al. 2022). This ultra-fine pozzolan reacts with the calcium hydroxide produced during cement hydration to form additional calcium silicate hydrate (C-S-H) (Al-Saffar et al. 2023). It results in a much denser and more refined microstructure, significantly reducing the permeability of the concrete. This dense matrix acts as a barrier against the penetration of sulphate ions, which are known to cause expansive chemical reactions leading to cracking and deterioration (Shannag and Shaia 2003). By minimising the entry of these harmful ions, silica fume prevents the formation of harmful compounds such as gypsum and ettringite, thus preserving the integrity of the concrete. In chloride-laden environments, such as coastal areas or areas where de-icing salts are used, the low permeability caused by silica fume is equally beneficial, as silica fume not only slows low chloride ingress but also increases the concrete's ability to chemically bind these ions, reducing their availability to initiate corrosion of steel reinforcement. This dual effect – as both a physical barrier and a chemical binder – makes silica fume an indispensable additive for concrete exposed to aggressive sulphate and chloride conditions (Ortega et al. 2018). Previous studies, listed in Table 1, have extensively investigated the effectiveness of silica fume in reducing sulphate and chloride attacks in concrete and have highlighted its fundamental role in enhancing the durability of the material. These studies used advanced analytical techniques such as scanning electron microscopy (SEM) and X-ray diffraction (XRD) to observe the microstructural changes and porosity reduction caused by silica fume. In addition, long-term exposure tests in aggressive environments confirmed the superior performance of silica fume-modified concrete, with results showing significantly lower sulphate-induced expansion and chloride-induced corrosion rates compared to conventional concrete (Sharaky et al. 2019). Understanding the mechanisms and effects of these attacks is crucial for engineers and builders aiming to increase the longevity and durability of concrete structures (Abed et al. 2018).

This article highlights the important role of using silica fume in cement mortars, especially in enhancing the fresh, physio-mechanical and durability of mortars subjected to high silica fume volume (up to 35%) and exposed to different concentration of NaCl and Na_2SO_4 conditions.

Table 1. Previous research related to the study.

Authors	Silica fume ratio (%)	Experiments	Optimum silica fume ratio found (%)
Saif Allah et al. (2024)	23, 46, 69	Compressive strength, Splitting tensile strength, Absorption test	69
Anwar (2005)	10	Compressive strength, Flexural strength, Pulse velocity, Dynamic elastic modulus	10
Kumar et al. (2022)	5,10, 15 (2.5%SF+2.5%FA, 5%SF+5%FA, 7.5%SF+7.5%FA)	Compressive strength, Splitting tensile strength, Water absorption	10 (with 7.5%SF+7.5%FA)
Şimşek et al. (2022)	0, 2.5, 5, 7.5, 10, 12.5, 15	Density, Setting time, Soundness, Compressive strength, Flexural strength	10
Ramezanianpour et al. (2020)	7.5 (with a natural pozzolan: 17.5)	Compressive strength, Capillary absorption, Penetration depth, Penetration profile, RCMT analysis, XRD analysis	7.5
Tripathi et al. (2020)	5, 10, 15, 20, 25	Fresh concrete properties, Compressive strength, Weight change	20
Sharaky et al. (2019)	5, 10, 15	Length expansion, Compressive strength, X-ray diffraction, DSC analysis, SEM analysis, EDX analysis	30
Abed et al. (2018)	0, 15, 25, 35	Compressive strength	25
Shetti and Das (2015)	1, 2, 3, 4, 5, 6	Slump, Compaction factor, Compressive strength, Acid attack, Water absorption, Chloride attack, Alkali attack	6
Lee et al. (2005)	5, 10, 15	Compressive strength	5, 10
Shannag and Shaia (2003)	0, 20, 40, 60 (+ natural pozzolan: 0, 5, 10, 15)	Compressive strength, UPV	15

2. Methodology

2.1. Materials

In this study, cement mortar samples were prepared using ordinary Portland cement (OPC) according to ASTM C150 (2024) was supplied by Amran Cement Plant. Specific gravity and fineness for cement were 3.15 g/cm^3 and 3140 cm^2/g. The used silica fume (SF) powder has a specific surface area of 20 m^2/g; it was sieved from a 75 μm sieve for eliminating large particles, an average diameter of 0.15 μm, silicon dioxide of 88.6%, and a specific gravity of 2.20 g/cm^3 (Fig. 1). Moreover, the chemical composition of both cement and silica fume is listed in Table 2.

Sand was used as a fine aggregate, and the specific gravity and water absorption were laboratory determined as 2.60 g/cm^3 and 1.40%, respectively.

Fig. 1. Silica fume.

Table 2. Chemical composition of the portland cement and silica fume.

Material	Oxide composition by mass (%)					
	SiO_2	CaO	MgO	Al_2O_3	Fe_2O_3	SO_3
Cement	23.2	55.1	2.2	7.4	5.4	2.0
Silica fume	88.6	0.99	0.26	1.11	0.66	0.33

2.2. Mix proportions, curing methods and sample preparation

In this study, based on the trial-and-error method to produce the best homogeneous, optimum cement dosage and W/B ratio, the control cement mortar sample was prepared as 1:1:0.45 for cement, fine aggregate, and water, respectively. A water reduction additive (superplasticizers (SPZ)) was used by a constant percentage (0.8%) of binder weight to increase mix workability. The other groups were prepared by replacing silica fume with 5%, 10%, 15%, 20%, 25%, 30%, and 35% by weight of cement. Table 3 shows the mixing ratios for each group.

Table 3. Mixture details and formulation code of the control and silica fume based mortar exposed to different solutions.

Group	Component weight (g)				
	Cement	Silica fume	Fine aggregate	SPZ	W/B
SF0	1000	--	1000	8	450
SF5	950	50	1000	8	450
SF10	900	100	1000	8	450
SF15	850	150	1000	8	450
SF20	800	200	1000	8	450
SF25	750	250	1000	8	450
SF30	700	300	1000	8	450
SF35	650	350	1000	8	450

Test samples were cured under five different conditions: water (laboratory conditions), 5% NaCl solution, 10% NaCl solution, 5% Na_2SO_4 solution, and 10% Na_2SO_4 solution, for 28 days. They were then air-dried for one day before testing.

2.3. Experiments

2.3.1. Slump test

In this study, the slump test was done according ASTM C143 (2020). This test is used for fresh concrete to determine the workability and percentage of water.

2.3.2. Density test

In this study, the average density of three samples in each group was calculated after 28 days. Samples were weighed with a sensitive electronic scale to an accuracy of 0.1 gm, and then density values (ρ) in g/cm^3 were calculated by dividing their mass (m) to their volume according to ASTM C642 (2021).

2.3.3. Ultra-sonic test (UPV)

The UPV test is a non-destructive technique used to evaluate the quality and integrity of mortar specimens. Sound's velocity through mortars gives details about their homogeneity, internal structure, and possible flaws. In this study, cubes with 50×50×50 mm^3 dimensions were directly measured for velocity as per ASTM C597 (2022) and using Eq. (1).

$$V = {}^{L}/_{T} \quad \text{(m/sec)} \tag{1}$$

2.3.4. Dynamic modulus of elasticity

In this study, the dynamic modulus of elasticity was calculated as per ASTM E494 (2020). For each sample and Eq. (2) were applied, then the average dynamic modulus of elasticity value was found for each group. Poisson's ratio of mortar was assumed as 0.17.

$$E_d = \frac{V_{\text{long}}^2 \cdot \rho \cdot (1+\nu) \cdot (1-2\nu)}{1-\nu} \tag{2}$$

where E_d is the dynamic modulus of elasticity, ρ is the mass density (g/cm^3), ν is the Poisson's ratio of mortar, and V_{long} is the speed rate of wave in specimen m/sec.

2.3.5. Capillary water absorption test

The capillary water absorption test was conducted in accordance with the standard ASTM C1585 (2020) after 28 days. The sides of the specimens were sealed with tape up to 20 mm in height so that only one face of the specimen was subjected to water. Water absorption measures were recorded from 2 min to 24 hr.

2.3.6. Compressive strength test

In this study, compression test was applied after 28 days by different curing methods (water, sodium sulfate and sodium chloride solve). The specimens were placed on a compression testing machine with a capacity of 2500 kN and a loading rate of 0.4 N/mm^2/sec, according to the ASTM C109 (2020). The load is applied gradually until the specimen fails. Stress-strain curved

were drawn and then, the modulus of elasticity, maximum compressive stress and strain values were calculated.

2.3.7. Flexural test

In this study, the flexural strength of prismatic beams (40×40×160 mm³) was obtained through a three-point bending (TPB) test based on the ASTM D790 (2017). A test machine of 50 kN with a controlled displacement rate of 0.2 mm/min was used. Average flexural strength values were measured at 28 days.

3. Results and Discussion

This study evaluated the fresh, physio-mechanical, and durability properties of mortars containing silica fume (up to 35%) under varying concentrations of NaCl and Na_2SO_4. The assessment included visual inspections, density measurements, ultrasonic pulse velocity, dynamic modulus of elasticity, capillary absorption, compressive strength, modulus of elasticity, and flexural tensile strength. The findings are systematically summarized in this section.

3.1. Slump

The results of the slump test were summarized in Table 4 and Fig. 2. Results clearly show that, as the amount of silica fume increases, the workability decreases. For the reference group (SF0), a 250 mm slump value was observed, and a linearly slight decrease was observed in the SF5, SF10, and SF10 groups. While a significant sudden drop was observed at SF20 to SF35 by 52% to 80%, respectively. Thus, silica fume particles with a high surface area require more water in combinations more than mixtures without silica fume.

Table 4. Physical and mechanical results.

Group	Slump (mm)	Density (kg/m³)	UPV test (m/sec)	Dynamic modulus of elasticity (GPa)	Flexural strength (MPa)
SF0	250	2,003.3	4,168.0	31.96	7.031
SF5	230	2,019.2	4,170.4	32.22	8.906
SF10	220	2,064.1	4,610.6	40.28	8.438
SF15	200	2,055.8	4,312.3	35.11	7.575
SF20	120	1,974.2	4,239.9	32.59	6.976
SF25	80	1,945.4	4,204.2	31.58	6.064
SF30	60	1,968.1	4,034.7	29.38	4.098
SF35	30	1,954.2	4,148.4	30.88	3.642

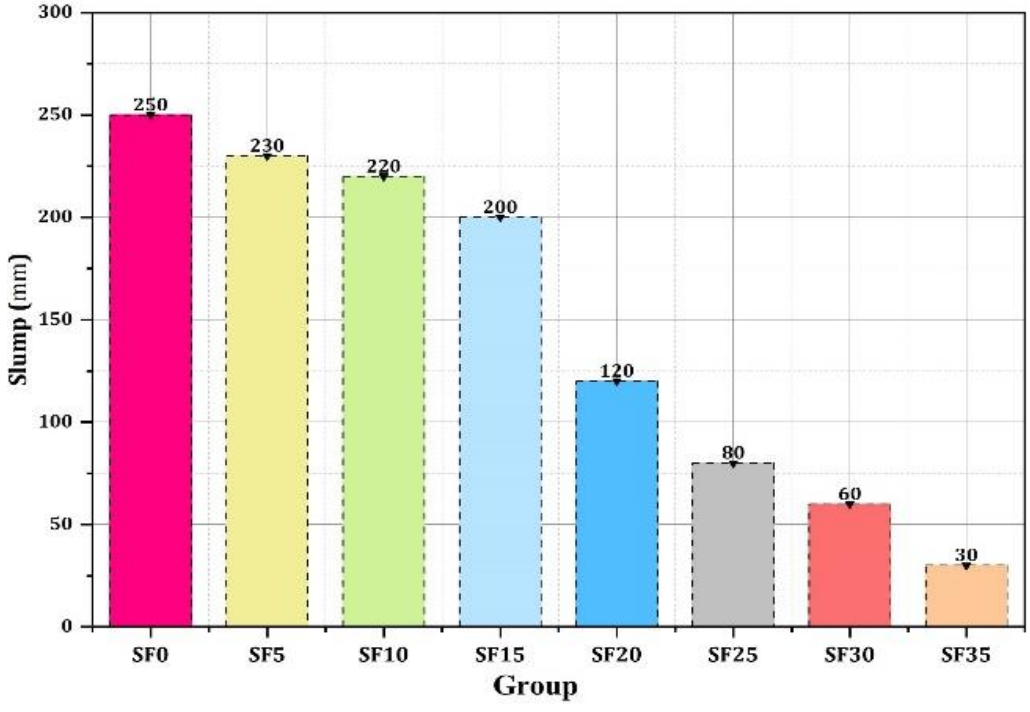

Fig. 2. Slump test results.

3.2. Density

The results of the density test on cement mortars with varying percentages of silica fume reveal a particular trend which indicates the effect of silica fume on the microstructure of the matrix. The density rises from 2.00 g/cm^3 with 0% silica fume to a maximum of 2.06 g/cm^3 with 10% silica fume. This is so because silica fume consists of ultrafine particles, it also fills in the cracks between cement bases or grains and makes more C-S-H, which effectively enhances the density. However, beyond 10%, the density begins to decline, with values dropping to 2.05 g/cm^3 at 15%, 1.98 g/cm^3 at 25%, and further to 1.95 g/cm^3 at 35% silica fume. The decline feature at higher percentages can be explained due to excessive fine nature of silica fume increasing the water demand hence poor workability and compaction uniformity. The findings indicate that silica fume densifies the composite up to an optimum amount of 10%. Beyond this amount, SiO_2 constitutes the mortar, which may lead to disruptions in homogeneity and segregation, making the mortar comparatively less dense.

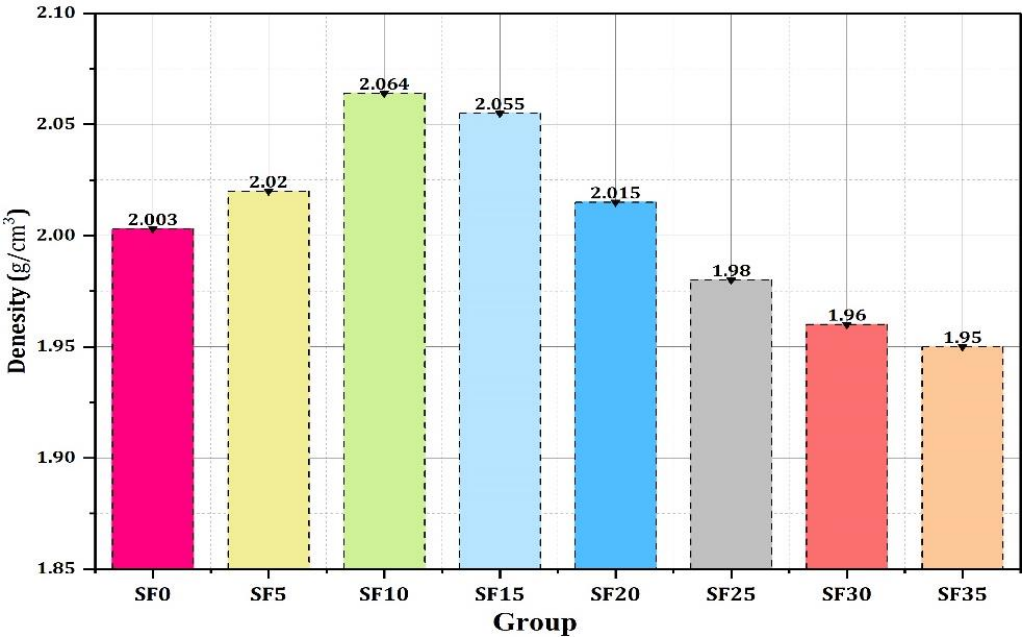

Fig. 3. Density test results.

3.3. Ultrasonic pulse velocity (UPV)

The results of UPV were listed in Table 4 and shown in Fig. 4. The UPV and density test results for cement mortars with varying silica fume contents show a parallel trend that highlights how microstructural changes affect both wave transmission and material density. Initially, both UPV and density increase, with UPV rising from 4168 m/s at 0% silica fume to a peak of 4610 m/s at 10%, and density increasing from 2.00 g/cm^3 to 2.06 g/cm^3 over the same range. This simultaneous rise in UPV and density indicates that up to 10% silica fume contributes to a denser, more uniform microstructure, likely due to improved particle packing and enhanced C-S-H formation through the pozzolanic reaction. This densification reduces porosity, allowing sound waves to travel faster and improving the mortar's structural integrity.

However, as silica fume content increases beyond 10%, both UPV and density begin to decline. UPV values drop from 4610 m/s to 4034 m/s at 30% silica fume, while density decreases from 2.06 g/cm^3 to 1.96 g/cm^3, indicating that higher silica fume levels may introduce microstructural inconsistencies. This parallel decline in UPV and density at higher silica fume levels underscores the importance of balanced silica fume content for enhancing both the material's structural integrity and wave propagation properties. Fig. 5 shows the correlation between UPV and density with R^2=0.657.

3.4. Dynamic modulus of elasticity

Fig. 6 and Table 4 show the dynamic modulus of elasticity results of each group. The results for the dynamic modulus of elasticity, UPV, and density tests for cement mortars for all groups containing silica fume exhibit a closely related trend that illustrates how micro structural densification influences each property. Initially, all three properties - dynamic modulus, UPV, and density - show an increase with silica fume addition up to 10%. The dynamic modulus rises from 31.9 GPa at 0% to a peak of 40.2 GPa at 10% silica fume, UPV increases from 4168 m/s to 4610 m/s, and density reaches its maximum at 2.06 g/cm^3. This parallel improvement suggests that up to 10% silica fume promotes a denser and more uniform matrix.

Beyond the 10% silica fume content, however, all three properties begin to decline, with the dynamic modulus dropping to 29.4 GPa at 30% silica fume, UPV falling to 4034 m/s, and density decreasing to 1.96 g/cm^3. This trend suggests that excess silica fume may negatively impact the compactness and uniformity of the matrix, likely due to reduced workability.

The alignment in the trends of dynamic modulus, UPV, and density indicates that around 10% silica fume is optimal for enhancing the mortar's overall physical and mechanical properties.

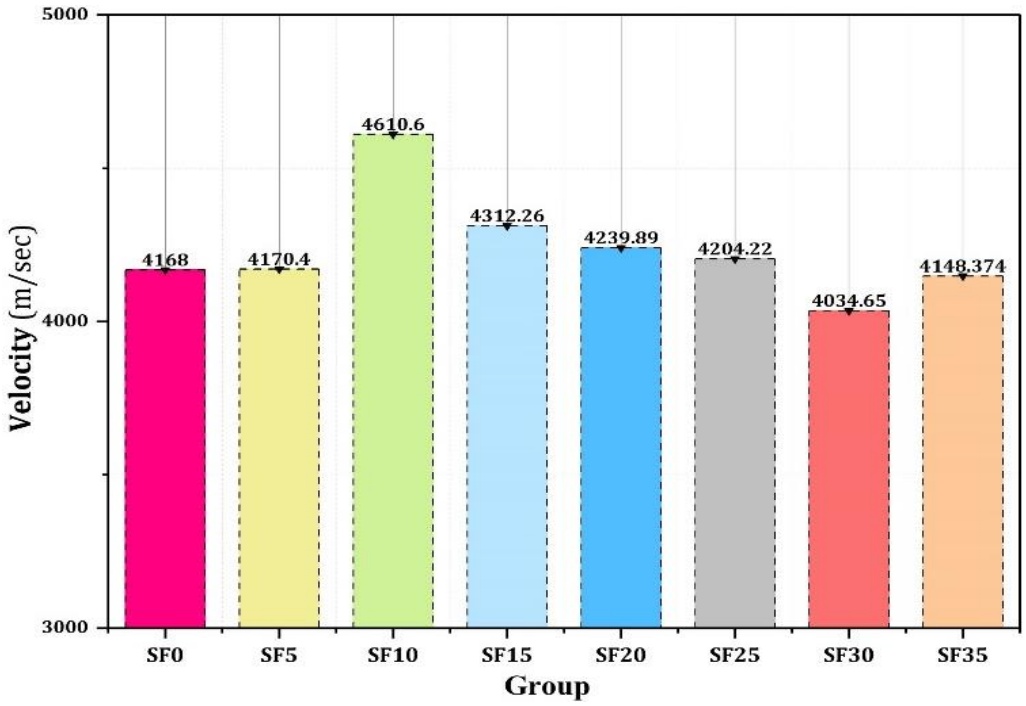

Fig. 4. UPV test results.

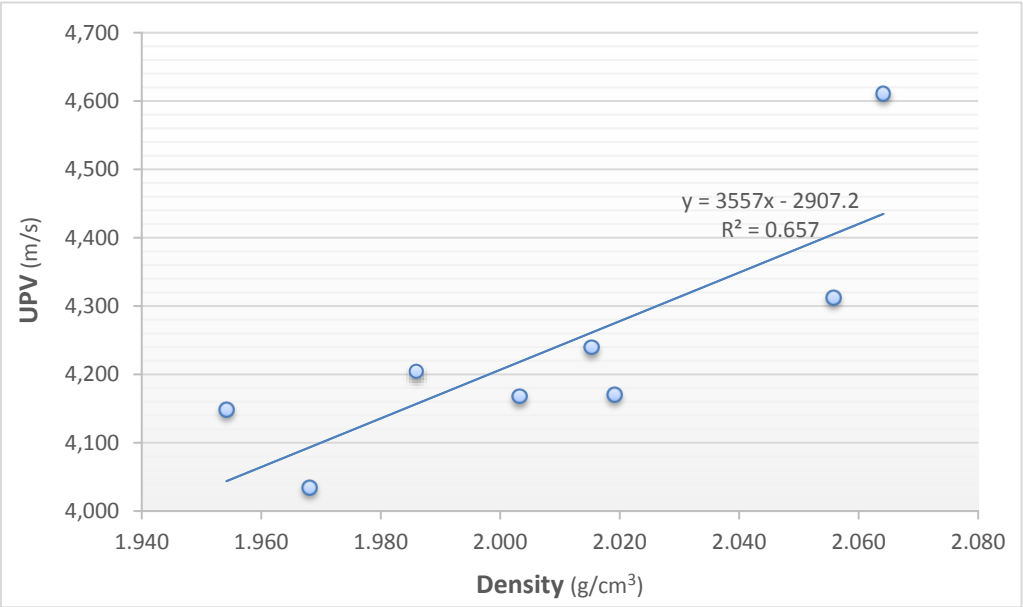

Fig. 5. Correlation between UPV and density.

3.5. Capillary absorption

Each point in Fig. 7 is the average value of measurements of three specimens. The capillary permeability of the mortar changed depending on the amount of SF. The graph shows an overall increasing trend in capillary rise with time for all samples. All the other samples (SF5 to SF35) show higher capillary rise at any given time compared to SF0. The highest increase is observed in FS35, with a 160%.

3.6. Compressive strength

The results of compressive strength for specimens cured in water, 5% NaCl solution, 10% NaCl solution, 5% Na_2SO_4 solution, and 10% Na_2SO_4 solution for 28 days were calculated as the average of three samples from each group, as shown in Table 5 and Figs. 8–10. The compressive strength results for all groups reveal a trend that aligns with observed changes in UPV and density, providing insight into how silica fume influences the

overall matrix strength and compactness. Initially, compressive strength increases sharply from 38 MPa at 0% silica fume to 53.1 MPa at 5%, reaching 46.8 MPa at 10%. This improvement mirrors the rise in both UPV (from 4168 m/s to 4610 m/s) and density (from 2.00 g/cm^3 to 2.06 g/cm^3) within the same range, indicating that the addition of silica fume enhances matrix densification. Up to 10% silica fume, the finer particles fill micro voids and engage in a pozzolanic reaction with calcium hydroxide to form additional C-S-H, which binds the matrix more effectively, increases compaction, and boosts strength.

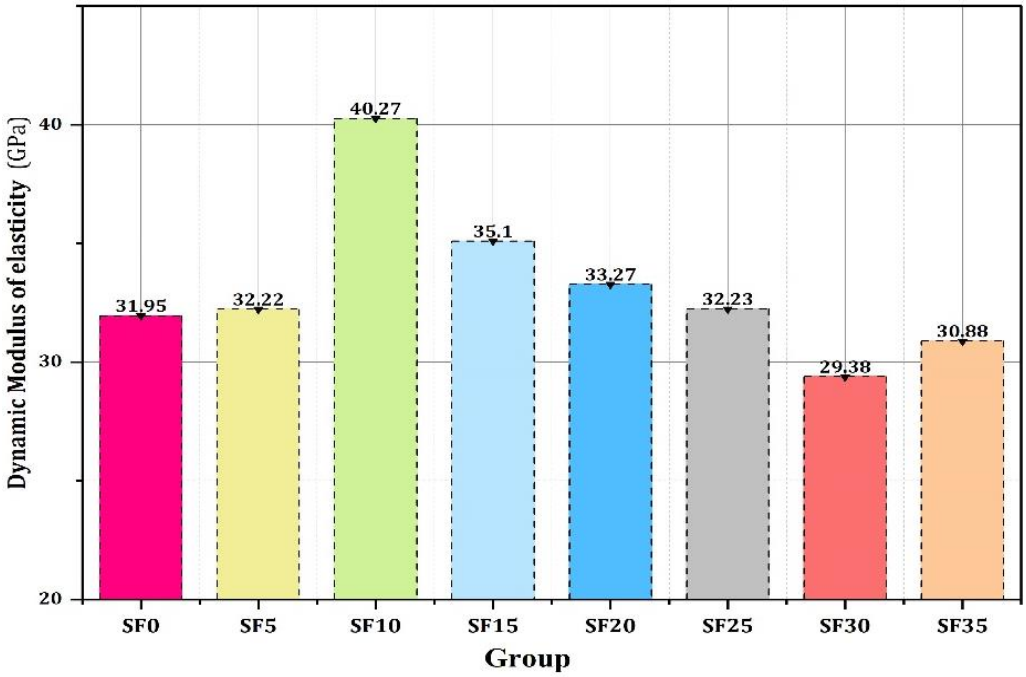

Fig. 6. Dynamic modulus of elasticity test results.

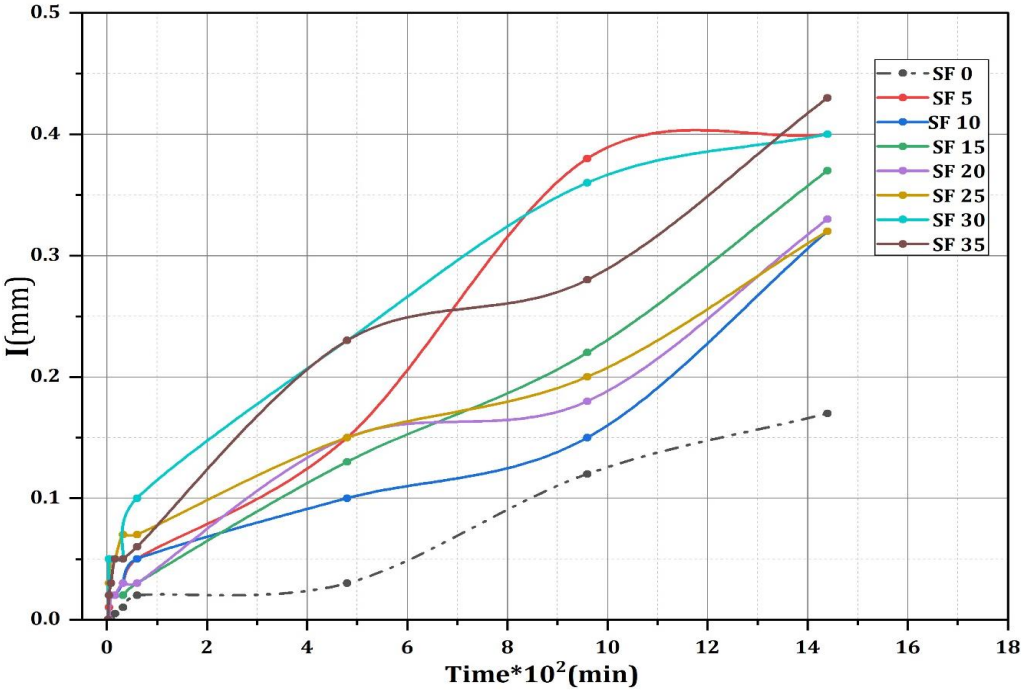

Fig. 7. Capillary test results.

Beyond 10% silica fume, compressive strength begins to decline, reaching 44.2 MPa at 15% and further decreasing to 36.8 MPa at 35%. This downward trend in compressive strength aligns with the reductions in UPV (dropping to 4034 m/s) and density (falling to 1.96 g/cm^3) observed at higher silica fume contents.

These results suggest that while adding silica fume around 5–10% enhances compressive strength by im-

proving microstructural densification hence higher silica fume contents lead to diminishing returns across all properties.

The compressive strength results for cement mortars cured in a 5% NaCl solution reveal a notable decrease for all silica fume groups compared to samples cured in water.

Compressive strength values drop from 38 MPa at 0% silica fume to 35 MPa, from 53.1 MPa at 5% to 39 MPa, and from 46.8 MPa at 10% to 36.6 MPa. This trend indicates that exposure to a saline environment adversely affects the mechanical properties, likely due to the corrosive effects of sodium chloride on the concrete matrix. The reductions in compressive strength are particularly pronounced at higher silica fume contents, with values decreasing to 32 MPa at 30% and 27.8 MPa at 35%, compared to 40.7 MPa and 36.8 MPa in the water-cured results.

The compressive strength results for cement mortars cured in a 10%NaCl solution demonstrate a further decline in strength across all silica fume content levels compared to the both water and 5%NaCl conditions. Specifically, compressive strength values decrease from 38 MPa at 0% silica fume to 34 MPa, from 53.1 MPa at 5% to 36.8 MPa, and from 46.8 MPa at 10% to 30.5 MPa. The decline in compressive strength is particularly significant at 10% and higher silica fume contents, where the strengths drop to 31.4 MPa at 15%, 31.5 MPa at 20%, 31.3 MPa at 25%, and 28.1 MPa at 35%.

The observed reductions in strength can be attributed to the higher concentration of sodium chloride intensifies the corrosive impact on the cement matrix, which can disrupt the formation and integrity of C-S-H and compromise the bond between the silica fume and the cement matrix. Additionally, the presence of NaCl at elevated concentrations may also induce internal stresses and microcracking, particularly in mortars with higher silica fume content, which are already predisposed to brittleness (Zhou et al. 2015).

Table 5. Compressive strength results.

Group	Compressive strength at 28 days (MPa)				
	Water	5% NaCl	10% NaCl	5% Na_2So_4	10% Na_2So_4
SF0	38.00	35.08	34.03	34.36	30.45
SF5	53.12	39.20	36.85	39.42	38.00
SF10	46.76	36.64	30.53	37.81	35.16
SF15	44.21	41.94	31.44	40.77	36.05
SF20	40.70	37.40	35.60	44.50	43.40
SF25	40.58	32.00	31.50	39.13	35.53
SF30	41.62	32.12	31.30	31.21	29.87
SF35	36.78	27.81	28.10	30.55	28.00

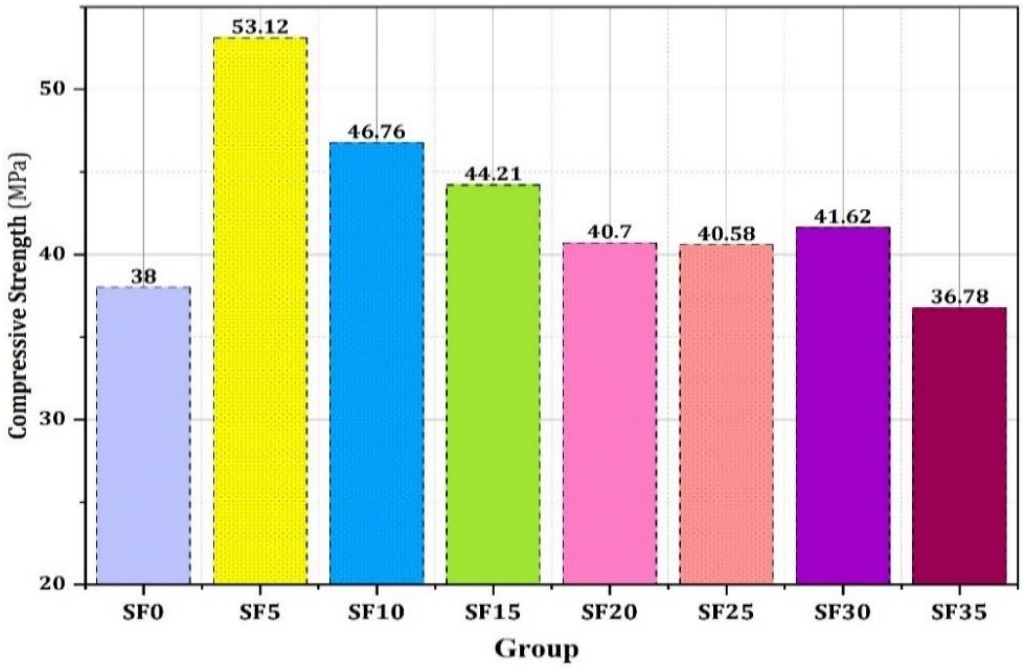

Fig. 8. Compressive strength results for the samples cured in water.

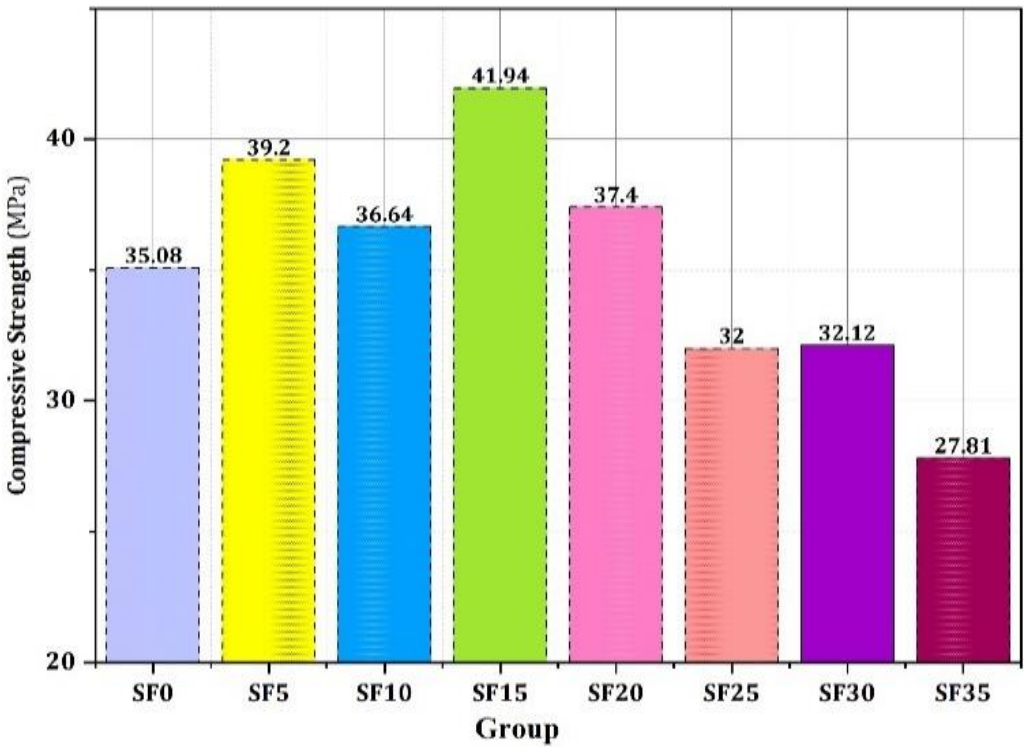

Fig. 9. Compressive strength results for the samples cured in 5% NaCl solution.

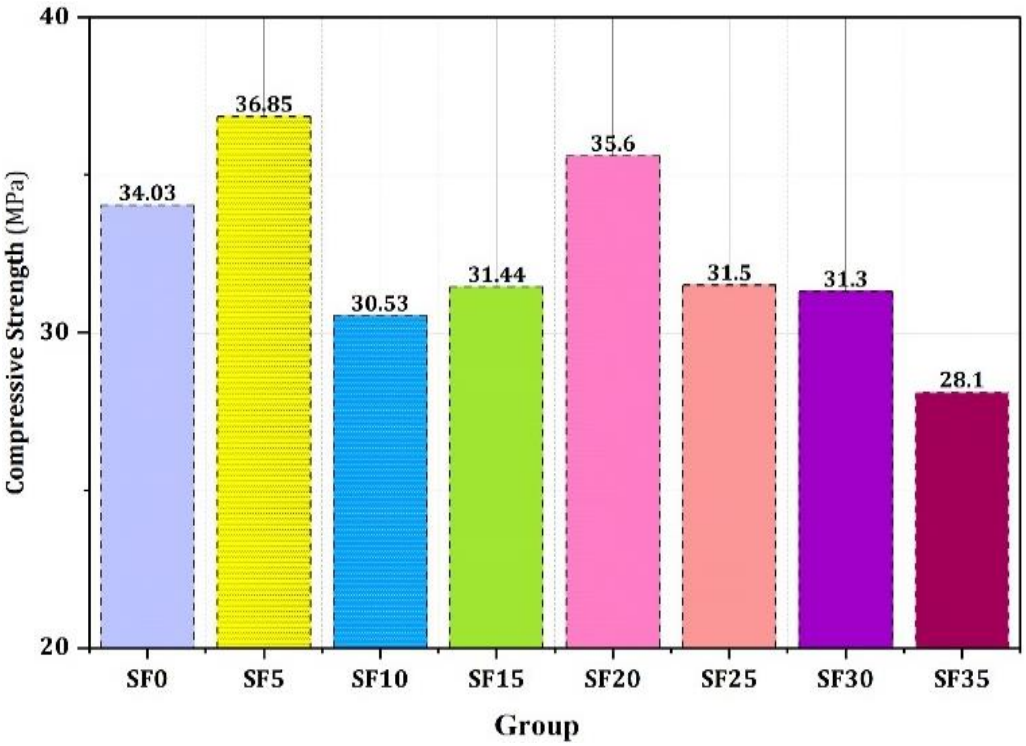

Fig. 10. Compressive strength results for the samples cured in 10% NaCl solution.

The compressive strength results for cement mortars cured in 5% and 10% Na_2SO_4 solutions reveal a significant decline in strength across all silica fume content levels compared to the compressive strengths obtained under water curing conditions (Figs. 11–12). In the 5% Na_2SO_4 solution, compressive strength values are recorded as 34.36 MPa at 0% silica fume, 39.4 MPa at 5%, 37.8 MPa at 10%, 40.77 MPa at 15%, 44.5 MPa at 20%, 39.13 MPa at 25%, 31.2 MPa at 30%, and 30.5 MPa at 35%. In comparison, the results for specimens cured in 10% Na_2SO_4 show further reductions, with compressive strengths of 30.4 MPa at 0%, 38 MPa at 5%, 35.2 MPa at 10%, 36.1 MPa at 15%, 43.4 MPa at 20%, 35.5 MPa at 25%, 29.8 MPa at 30%, and 28 MPa at 35%.

The initial decline in compressive strength in the 5% Na_2SO_4 solution compared to water-cured specimens

reflects the detrimental effects of sulfate ions, which can react with the hydration products in cement, potentially leading to the formation of expansive products such as ettringite. This expansive reaction may create internal stresses within the mortar matrix, promoting cracking and reducing overall strength. The further decrease in compressive strength observed in the 10% Na_2SO_4 solution suggests that higher sulfate concentrations exacerbate these effects, leading to increased permeability and more significant microstructural damage (Han and Li 2024). Notably, while some mortars, particularly those with 20% silica fume, show relatively higher strength retention in both sulfate solutions compared to others, the overall trend emphasizes the vulnerability of silica fume-enhanced mortars to Na_2SO_4 attack.

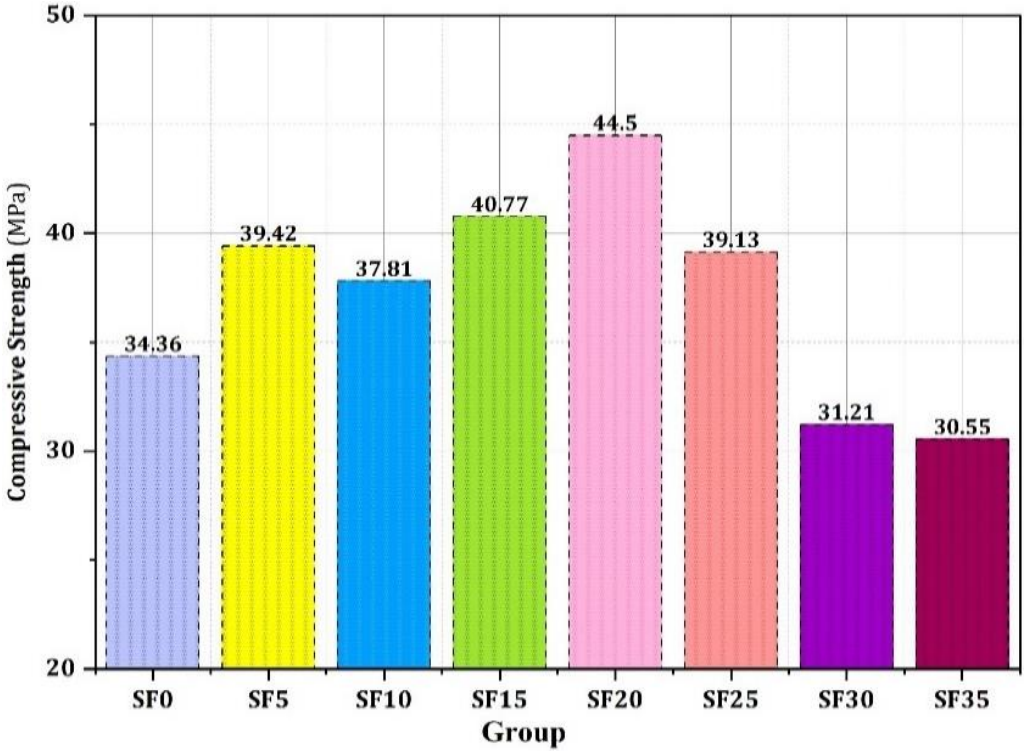

Fig. 11. Compressive strength results for the samples cured in 5% Na_2So_4 solution.

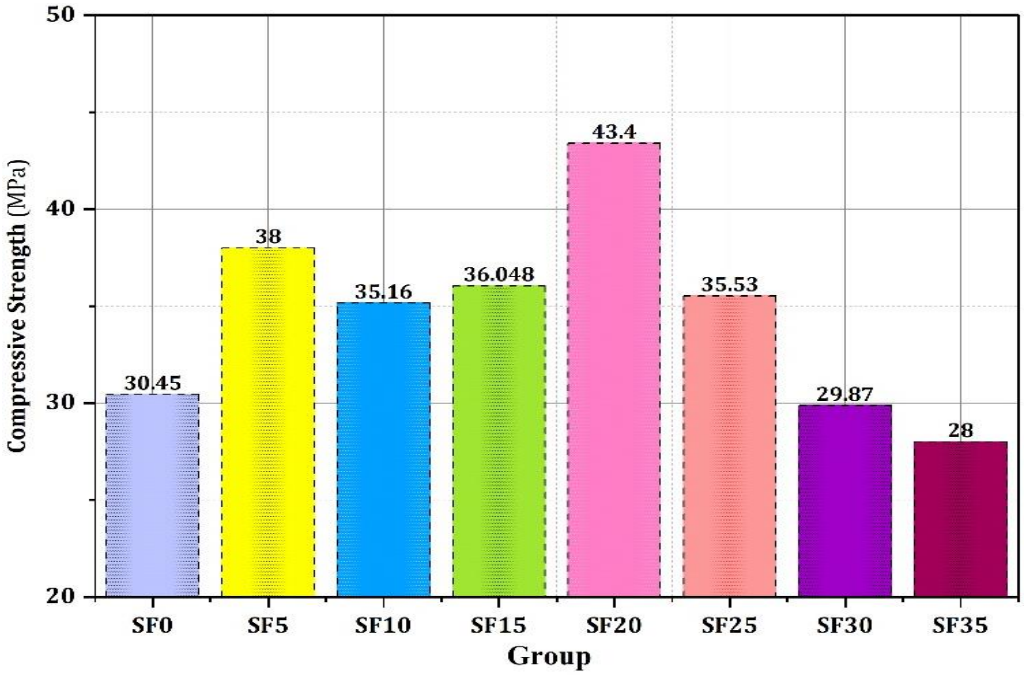

Fig. 12. Compressive strength results for the samples cured in 10% Na_2So_4 solution.

3.7. Modulus of elasticity

Table 6 summarizes the results of modulus of elasticity and Figs. 13–17 show the stress-strain curves under compression for all curing methods. The modulus of elasticity results reflects significant differences based on the curing conditions, showcasing how aggressive environmental factors influence the mechanical behaviour. For specimens cured in water, the modulus values range from 4.3 GPa at 0% silica fume to a peak of 12.3 GPa at 10%. The optimal hydration conditions provided by water curing facilitate the pozzolanic reaction, allowing the silica fume to effectively contribute to the matrix's strength and elasticity.

In contrast, when the specimens are cured in a 5% Na_2SO_4 solution, the modulus values drop significantly, ranging from 3.3 GPa at 0% silica fume to 9.3 GPa at 15%. The decline in modulus continues to be pronounced in specimens cured in a 10% Na_2SO_4 solution, with values ranging from 3.1 GPa at 0% silica fume to a maximum of only 8.4 GPa at 15%. The formation of ettringite and other expansive products is likely intensified, leading to greater microstructural damage and a more significant loss of elasticity.

Comparatively, the results from specimens cured in saline environments exhibit similar downward trends in modulus of elasticity. In the 5% NaCl-cured specimens, modulus values range from 4.8 GPa at 0% silica fume to 6.6 GPa at 15%. Although the modulus is higher than that observed in the sulphate-cured specimens, the presence of sodium chloride still negatively impacts the mortar's stiffness.

Finally, the lowest modulus values are recorded for specimens cured in a 10% NaCl solution, where results range from 3.4 GPa at 0% silica fume to 4.98 GPa at 20%. The decline in modulus compared to both water-cured and 5% NaCl specimens suggests that the higher concentration of chloride exacerbates the detrimental effects on the mortar's mechanical properties. The increased salinity may enhance the likelihood of microcracking and reduce the overall elastic behaviour of the mortar.

Table 6. Modulus of elasticity results.

Group	Modulus of elasticity at 28 days (GPa)				
	Water	5% NaCl	10% NaCl	5% Na_2So_4	10% Na_2So_4
SF0	4.34	4.77	3.41	3.29	3.13
SF5	11.91	4.42	3.55	5.54	8.84
SF10	12.33	5.36	4.14	4.95	5.33
SF15	9.70	6.60	3.22	9.30	3.74
SF20	9.63	6.40	4.98	8.36	8.40
SF25	7.46	5.05	3.80	7.28	3.76
SF30	9.50	3.67	3.54	4.66	2.70
SF35	8.71	3.37	3.27	4.00	3.52

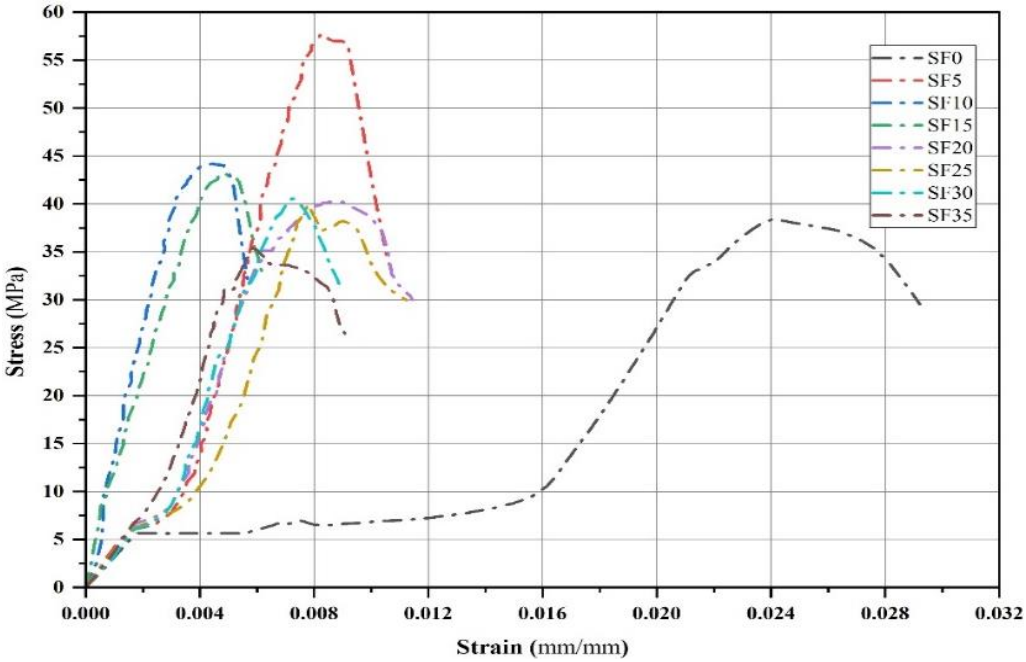

Fig. 13. Stress-strain curve for the groups cured in water.

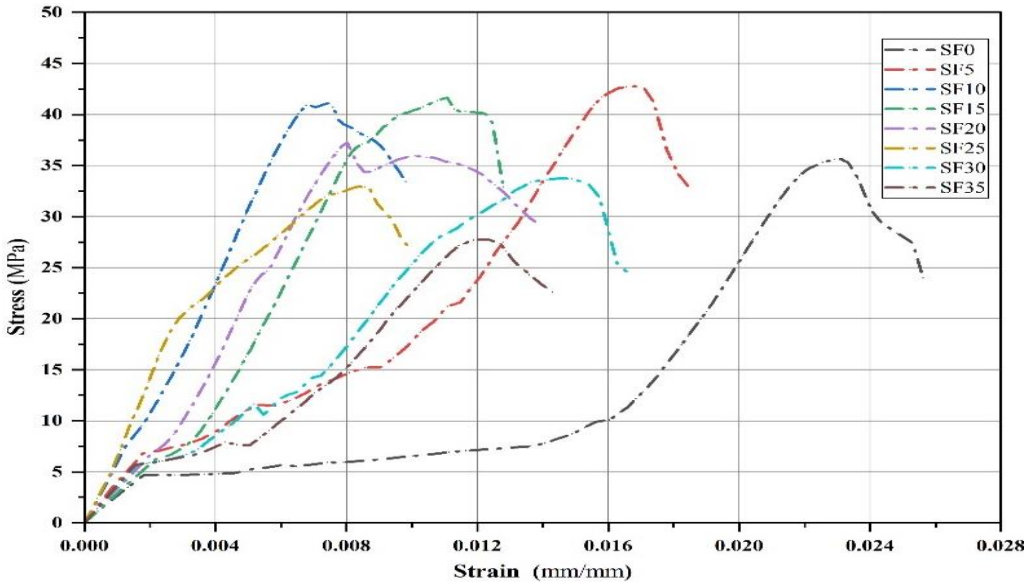

Fig. 14. Stress-strain curve for the groups cured in 5% NaCl solution.

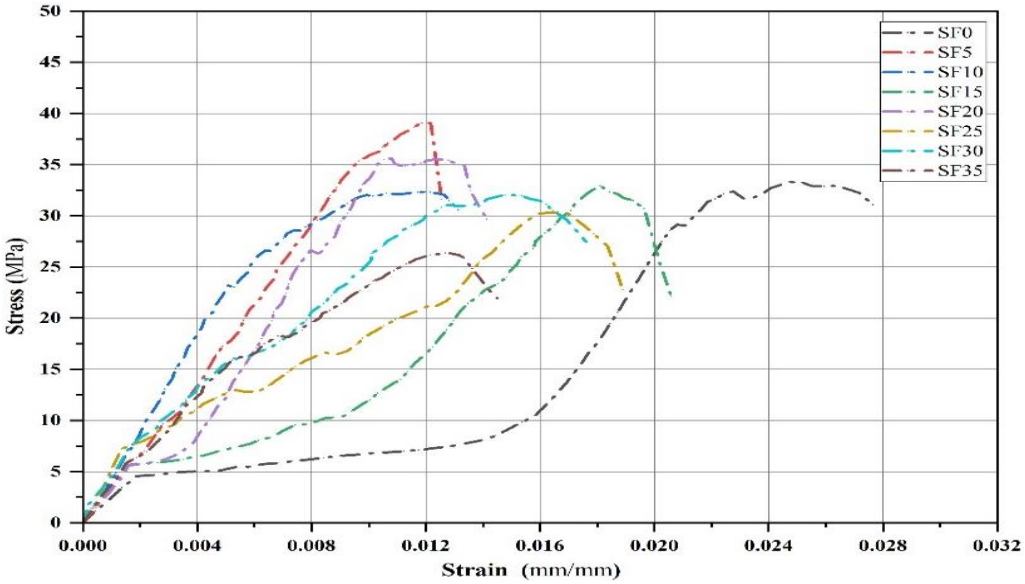

Fig. 15. Stress-strain curve for the groups cured in 10% NaCl solution.

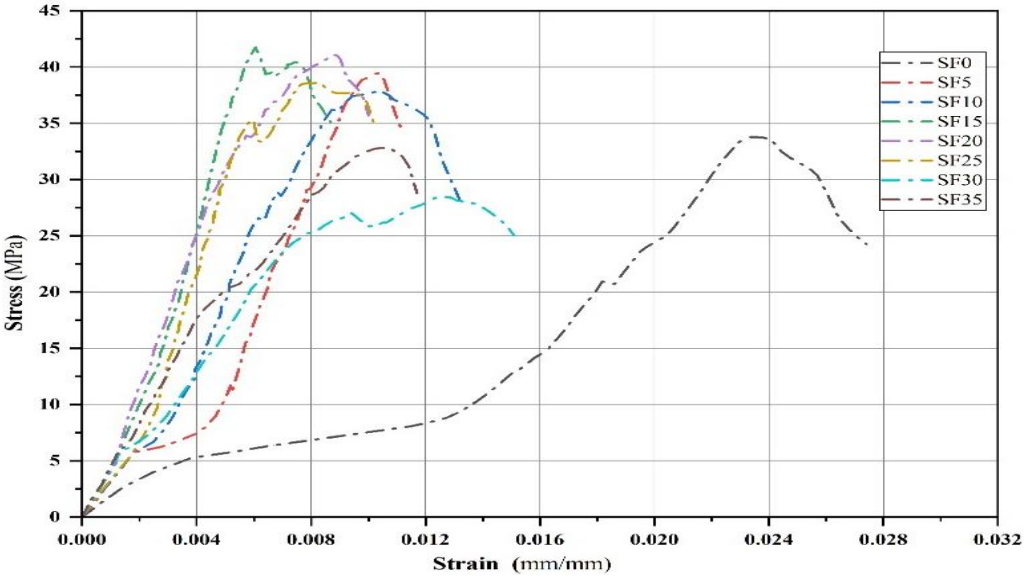

Fig. 16. Stress-strain curve for the groups cured in 5% Na_2So_4 solution.

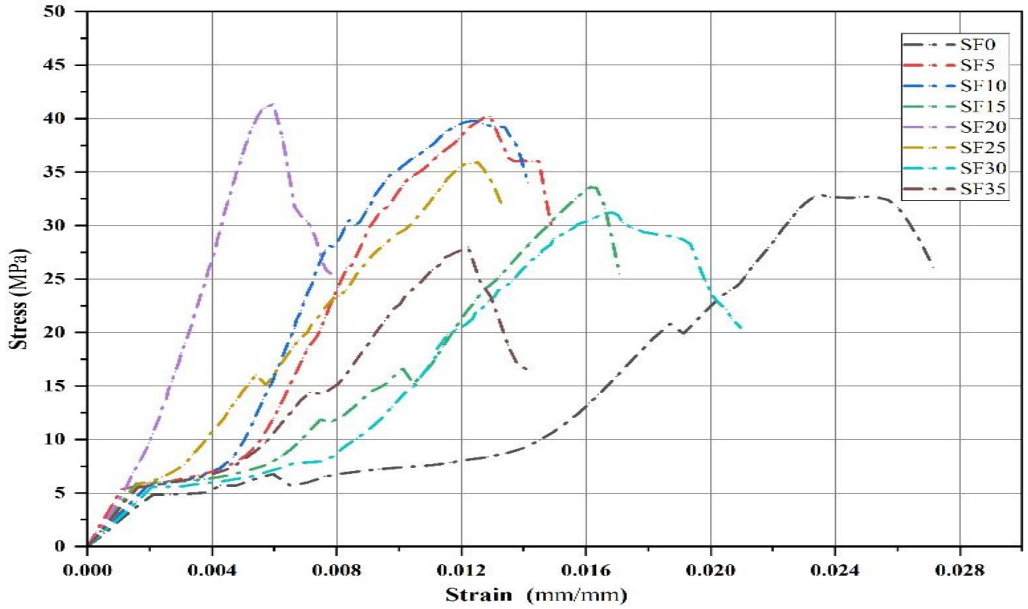

Fig. 17. Stress-strain curve for the groups cured in 10% Na_2So_4 solution.

3.8. Flexural strength

The results of flexural test for specimens submerged in water were calculated as the average of three samples from each group as shown in Fig. 18. The flexural strength results for cement mortars with varying silica fume contents indicate a moderate performance under normal curing conditions, with values ranging from 7.03 MPa at 0% silica fume to a peak of 8.91 MPa at 5%. However, the observed decline in flexural strength at higher silica fume contents, specifically at 10% (8.44 MPa), 15% (7.6 MPa), and beyond, suggests that excessive silica fume may lead to a more brittle mix with reduced flexural capacity.

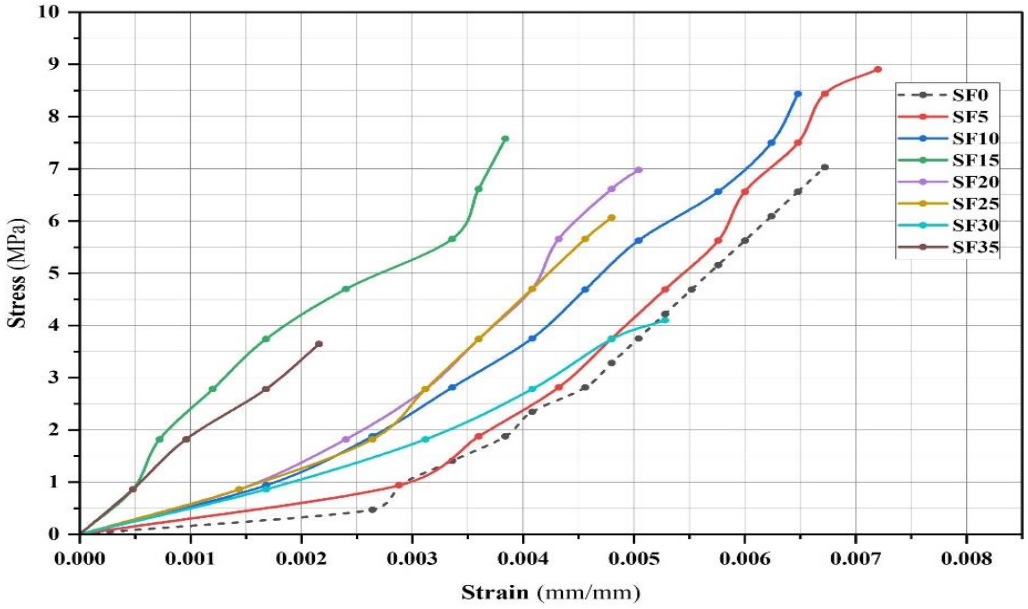

Fig. 18. Stress-strain curve for the water cured samples in 3-point test.

Furthermore, the decrease in flexural strength at higher silica fume levels is also supported by the lower values observed at 20% (6.98 MPa), 25% (6.06 MPa), 30% (4.1 MPa), and 35% (3.64 MPa). These results indicate a significant reduction in the material's ability to withstand bending stresses, highlighting the diminishing returns of silica fume as a partial replacement for cement. The increased brittleness at higher percentages may be due to the high silica fume content creating a dense, but less flexible, structure that is more susceptible to crack propagation under load (Hamada et al. 2023).

The maximum flexural strength of 8.91 MPa at 5% silica fume corresponds with a compressive strength peak of 53.1 MPa under similar water curing conditions, highlighting how the optimal silica fume content can enhance both properties effectively.

However, as the silica fume content increases beyond 5%, a notable decline in both flexural and compressive strengths occurs, particularly at 10% (8.44 MPa flexural) and 15% (7.6 MPa flexural), which correlates with a decrease in compressive strength (46.8 MPa and 40.7 MPa, respectively). This trend suggests that while moderate amounts of silica fume enhance strength, excessive content can lead to increased brittleness and reduced ductility, impacting the material's overall performance under both compressive and flexural loads (Lou et al. 2023).

The lower flexural strength values observed at higher silica fume levels, such as 6.98 MPa at 20% and 3.64 MPa at 35%, correspond with significant drops in compressive strength, indicating that the microstructural integrity may be compromised due to the high pozzolanic content.

4. Conclusions

This study aimed to investigate the effects of varying silica fume contents on cement mortar properties, including compressive strength, flexural strength, modulus of elasticity, and UPV, under different curing conditions. The findings provide insight into the effectiveness of silica fume as a partial cement replacement and highlight the importance of environmental factors in determining the performance of these mortars. The following points are highlighted:

- Peak compressive strength of 53.1 MPa was observed at 5% silica fume content under water curing, indicating enhanced strength due to improved microstructure, while a general decline in compressive strength was noted at higher silica fume levels, with values dropping to 36.8 MPa at 35%, suggesting increased brittleness and microcracking at excessive silica fume contents.
- Flexural strength reached a maximum of 8.91 MPa at 5% silica fume, correlating with the highest compressive strength, which emphasizes the role of silica fume in enhancing ductility. While a significant reduction in flexural strength was noted at higher percentages, with values falling to 3.64 MPa at 35%, reflecting the negative impact of excessive silica fume on the material's ability to resist bending.
- The modulus of elasticity peaked at 12.3 GPa for the water-cured specimens at 10% silica fume, supporting the enhanced stiffness observed with optimal silica fume levels. While exposure to harmful environments, such as 5% and 10% Na_2SO_4 and NaCl solutions, led to substantial decreases in modulus values, with the lowest recorded at 2.7 GPa in 10%Na_2SO_4, indicating significant degradation of the material's mechanical properties.
- The compressive and flexural strengths, as well as modulus values, significantly declined in saline and sulphate environments, highlighting the vulnerability of silica fume-enhanced mortars to chemical attack.
- Results showed that while silica fume can enhance performance, excessive content in harmful environments can lead to severe reductions in mechanical properties, emphasizing the need for careful material design.

In addition, recommendations for the further research could be summarized as following:

- Conduct long-term exposure tests to evaluate the durability of silica fume-enhanced mortars in aggressive environments over extended periods.
- Perform detailed microstructural investigations using techniques such as scanning electron microscopy (SEM) or X-ray diffraction (XRD) to better understand the interactions between silica fume and cementitious materials.
- Investigate the effectiveness of protective coatings or sealers that could enhance the resistance of silica fume mortars to chemical attacks, such as saline and sulphate environments.
- Assess the behaviour of silica fume-enhanced mortars under various loading conditions.
- Conduct a cost-benefit analysis of incorporating silica fume in cementitious materials to determine its economic advantages.

Acknowledgements
None declared.

Funding
The authors received no financial support for the research, authorship, and/or publication of this manuscript.

Conflict of Interest
The authors declared no potential conflicts of interest with respect to the research, authorship, and/or publication of this manuscript.

Author Contributions
All of the authors made substantial contributions to conception and design, or acquisition of data, or analysis and interpretation of data; were involved in drafting the manuscript or revising it critically for important intellectual content; and gave final approval of the version to be published.

Data Availability
The datasets created and/or analyzed during the current study are not publicly available, but are available from the corresponding author upon reasonable request.

References

Abed M, Nasr M, Hasan Z (2018). Effect of silica fume/binder ratio on compressive strength development of reactive powder concrete under two curing systems. *MATEC Web of Conferences*, 162, 02022.

Alameri I, Oltulu M, Ardahanlı M (2020). Influence of preheating on the mechanical properties of high strength concrete with micro silica filler. *Bilecik Seyh Edebali University Journal of Science*, 7(2), 1084-1093.

Al-Saffar FY, Wong LS, Paul SC (2023). An elucidative review of the nanomaterial effect on the durability and calcium-silicate-hydrate (CSH) gel development of concrete. *Gels*, 9(8), 613.

Anwar M (2005). Effect of cementitious materials on concrete against sulfate attack. *Engineering Research Journal*, 99, C92-C104.

ASTM C109/C109M-20 (2020). Standard test method for compressive strength of hydraulic cement mortars (using 2-in. or [50-mm] cube specimens). ASTM International, West Conshohocken, PA.

ASTM C143/C143M-20 (2020). Standard test method for slump of hydraulic-cement concrete. ASTM International, West Conshohocken, PA.

ASTM C150/C150M-24 (2024). Standard specification for portland cement. ASTM International, West Conshohocken, PA.

ASTM C597-22 (2022). Standard test method for ultrasonic pulse velocity through concrete. ASTM International, West Conshohocken, PA.

ASTM C642-21 (2021). Standard Test method for density, absorption, and voids in hardened concrete. ASTM International, West Conshohocken, PA.

ASTM C1585-20 (2020). Standard test method for measurement of rate of absorption of water by hydraulic-cement concretes. ASTM International, West Conshohocken, PA.

ASTM D790-17 (2017). Standard test methods for flexural properties of unreinforced and reinforced plastics and electrical insulating materials. ASTM International, West Conshohocken, PA.

ASTM E494-20 (2020). Standard practice for measuring ultrasonic velocity in materials by comparative pulse-echo method. ASTM International, West Conshohocken, PA.

Atabey İ, Çelikten S, Canbaz M (2023). Chemical resistance of hardened mortar containing andesite and marble industry waste powder. *Challenge Journal of Concrete Research Letters*, 14(2), 31-38.

Atasever M, Tokyay M (2024). Determining datum temperature and apparent activation energy: an approach for mineral admixtures incorporated cementitious systems. *Challenge Journal of Concrete Research Letters*, 15(4), 142-149.

Feng L, Zhao P, Wang Z, Gao J, Su X, Li H (2018). Improvement of mechanical properties and chloride ion penetration resistance of cement pastes with the addition of pre-dispersed silica fume. *Construction and Building Materials*, 182, 483-492.

Güney B, Yıldızel S (2024). Optimization of mechanical properties in lime-based composites using the Taguchi method. *Challenge Journal of Structural Mechanics*, 10(3), 109-115.

Hamada HM, Abed F, Katman HYB, Humada AM, AlJawahery MS, Majdi A, Yousif ST, Thomas BS (2023). Effect of silica fume on the properties of sustainable cement concrete. *Journal of Materials Research and Technology*, 24, 8887-8908.

Han M, Li J (2024). Enhancement of compressive strength and durability of sulfate-attacked concrete. *Buildings*, 14(7), 2187.

Harirchian E (2024). Predicting compressive strength of AAC blocks through machine learning advancements. *Challenge Journal of Concrete Research Letters*, 15(2), 56-68.

Lee, FH, Lee Y, Chew SH, Yong KY. (2005). Strength and modulus of marine clay-cement mixes. *Journal of Geotechnical and Geoenvironmental Engineering*, 131(2), 178–186.

Lou Y, Khan K, Amin MN, Ahmad W, Deifalla AF, Ahmad A (2023). Performance characteristics of cementitious composites modified with silica fume: A systematic review. *Case Studies in Construction Materials*, 18, e01753.

McCarthy MJ, Dyer TD (2019). Pozzolanas and pozzolanic materials. *In: Hewlett PC, Liska M, editors*. Lea's Chemistry of Cement and Concrete (5th edition), Butterworth-Heinemann, Oxford, United Kingdom, 363-467.

Ortega JM, Esteban MD, Williams M, Sánchez I, Climent MÁ (2018). Short-term performance of sustainable silica fume mortars exposed to sulfate attack. *Sustainability*, 10(7), 2517.

Ramezanianpour, AA, Riahi Dehkordi E, Ramezanianpour AM (2020). Influence of sulfate ions on chloride attack in concrete mortars containing silica fume and jajrood trass. *Iranian Journal of Science and Technology, Transactions of Civil Engineering*, 44(4), 1135–1144.

Saif Allah JS, Kassim MM, Salman GA (2024). The durability of concrete mortars with different mineral additives exposed to sulfate attack. *Salud, Ciencia y Tecnología - Serie De Conferencias*, 3, 851.

Shannag M, Shaia HA (2003). Sulfate resistance of high-performance concrete. Cement and Concrete Composites, 25(3), 363-369.

Sharaky IA, Megahed FA, Seleem MH, Badawy AM (2019). The influence of silica fume, nano silica and mixing method on the strength and durability of concrete. *SN Applied Sciences*, 1(6), 575.

Shetti, AP, Das BB. (2015). Acid, alkali and chloride resistance of early age cured silica fume concrete. *In: Matsagar V, editor.* Advances in Structural Engineering. Springer India, New Delhi, India, 1849-1862.

Şimşek O, Aruntaş HY, Demir İ, Yaprak H, Yazıcıoğlu S (2022). Investigation of the effect of seawater and sulfate on the properties of cementitious composites containing silica fume. *Silicon*, 14(2), 663–675.

Tripathi D, Kumar R, Mehta PK, Singh A (2020). Silica fume mixed concrete in acidic environment. *Materials Today: Proceedings*, 27, 1001–1005.

Zhou ZY, Gencturk B, Willam K, Attar A (2015). Carbonation-induced and chloride-induced corrosion in reinforced concrete structures. *Journal of Materials in Civil Engineering*, 27(9), 04014245.